Flexible Carbon Nanotube Hydrogen Gas Sensor based on PET Substrate

AHMAD M. AL-DIABAT[1,*], NATHEER A. ALGADRI[2], NASER M. AHMED[3], TARIQ ALZOUBI[4], GHASEB N. MAKHADMEH[5], ABDULSALAM ABUELSAMEN[6], OSAMA ABU NOQTA[7], AMAL MOHAMED AHMED ALI[8]

[1]Department of Physics, Al-Zaytoonah University of Jordan,
Amman,
JORDAN

[2]Department of Physics, Isra University,
Amman,
JORDAN

[3]Department of Laser and Optoelectronics Engineering, Dijlah University College,
Baghdad,
IRAQ

[4]College of Engineering and Technology, American University of the Middle East,
Egaila, 54200,
KUWAIT

[5]General Education Department, Skyline University College,
Sharjah, P.O. Box 1797,
UAE

[6]Medical Imaging and Radiography Department, Aqaba University of Technology,
Aqaba 910122,
JORDAN

[7]MEU Research Unit, Middle East University,
Amman 11831,
JORDAN

[8]Prince Sattam Bin Abdulaziz University,
Alkharj 11942,
SAUDI ARABIA

**Corresponding Authors*

Abstract: - This study presents a cost-effective and straightforward approach for fabricating a highly effective sensor to hydrogen (H_2) gas using carbon nanotubes (CNTs), which were synthesized by a conventional microwave oven. To optimize CNT properties, a series of five purification processes were employed to eliminate impurities such as metal particles and support material from the carbon nanotubes produced. Then CNT was deposited onto a polyethylene thermal (PET) substrate through the application of a dielectrophoretic method. The gas sensors which fabricated have many significant exceptional characteristics, including high flexibility, remarkable conformability, and cost-effectiveness. The carbon nanotubes (CNTs) demonstrated significant sensitivity when exposed to H_2 gas at room temperature (RT). At a concentration of 140 parts per million (ppm) of H_2, the CNTs exhibited a remarkable sensitivity of up to 15%.

Key-Words: - CNT, Hydrogen, PET gas sensor, microwave, flexible, nanotube, microwave, room temperature, sensitivity.

Received: April 25, 2025. Revised: August 9, 2025. Accepted: September 23, 2025. Published: December 17, 2025.

1 Introduction

Investigation on the use of CNTs as gas sensors originated twenty years ago, [1], [2]. Two types of CNT are based on the wrapping of graphene sheets in the axial direction: single-walled carbon nanotubes (SWCNTs) and multi-walled carbon nanotubes (MWCNTs). It is noted that one sheet wherein every atom acts as a shell atom in SWCNTs, whereas there are several sheets in the case of MWCNTs, [3]. The production of nanotubes is expensive and still presents challenges, mainly because of the difficulty in growing continuously long, structurally perfect tubes, [4], [5].

Carbon nanotubes are chemically and mechanically stable and have good electronic properties for making them a good candidate for gas sensing. They also have with high surface/volume ratio, [6], [7]. These sensors belong to the new generation that may have a large perspective on the gas sensing market. Carbon nanotubes (CNTs) are known to be sensitive to gases with high electron-withdrawing or -donating nature, such as ammonia (NH_3), nitrogen dioxide (NO_2), and hydrogen (H_2), [8], [9].

One of the ultimate intentions of gas sensors is to protect and maintain safety and security. Work on H2 gas sensors [10] is indispensable in all domains related to a rapidly emerging hydrogen economy, where hydrogen gas is used as an energy carrier and chemical reagent. Researchers have investigated the application of NiO as a p-type semiconducting material in nanowires for hydrogen gas sensing in recent studies. These studies have provided encouraging results, [6]. The conductivity of curvilinear sensors is governed by several important factors, such as the aspect ratio, surface area, and percolation of the conductive nanomaterials. As a result, the flexible sensors made of high aspect ratio carbon nanotubes (CNTs) have shown superior conductive and tensile properties, with an obtained conductivity of 53 S cm-1 and a tensile strain of 38%. The value provided is 75.

The conductivity of the present sensors was 500 times as high as that of flexible sensors, which had a lower aspect ratio of 0.1 S cm-1. Further examples of bulk nanomaterials, carbon-based, include multi-wall carbon nanotubes (MWCNTs), [11], [12]. Due to their remarkable properties like high surface area, low specific weight, and excellent conductivity, carbon and metal nanoparticles have become very promising candidates to improve the mechanical and conductivity of flexible sensors, [10].

[13] reported the development of a gas detector utilizing multi-walled carbon nanotubes. The findings indicated a sensitivity of approximately 12.3% when exposed to 4000 ppm of H2 gas at RT. Additionally, the response time was measured to be 200 seconds. They reported a gas sensor based on multi-walled carbon nanotubes. The results showed a sensitivity of 12.3% for 4000 ppm H2 gas at RT. The response time was also found to be 200s. Also, Shrivastava, [14] prepared H2 gas sensors based on multiwall carbon nanotubes. Can we schedule a meeting between ourselves to follow up on the next project at 500 ppm of H2 gas, the sensors showed a sensitivity of 2.1% and a response time of 150 s.

The originality of this work lies in the application of commercial dielectrophoretic (DEP) deposition of CNTs on a PET substrate. The proposed method is proven to possess superior gas sensing performance, including good sensitivity at lower operation temperature, shorter recovery time, enhanced sensitivity to low gas concentration, and much faster response speed in the open air. The CNT-based sensor showed good reversible and reproducible sensing behaviours to hydrogen (H2) at room temperature over a period of 55 min. The recording-enhanced CNT performance can be explained mainly as a result of the high surface-to-volume ratio of CNTs and the improved H adsorption on the surface of functional CNTs. Based on the proposed fabrication process and the utilization of ultra-sensitive carbon nanotubes (CNTs), the cost and operating power consumption can be greatly reduced for the hydrogen gas sensor.

2 Experimental Part

2.1 Synthesised CNT

The CNTs were synthesized by the conventional microwave oven method. Figure 1 shows the combined graphite and ferrocene that was compressed in quartz boats with a graphite: ferrocene ratio of 70:30 to achieve a uniform microwave heat distribution throughout the entire quartz boat. The microwave was abruptly turned off when a spark was detected, [15].

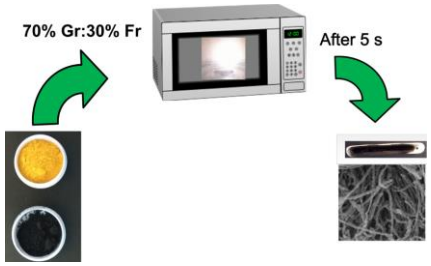

Fig. 1: Synthesis of CNT using a microwave oven
Source: [15]

2.2 Carbon Nanotube Treatment

One gram of as-synthesized carbon nanotubes (A-CNT) was treated in 1 liter of nitric acid (2.6 M HNO_3) with stirring and ultrasonication at room temperature for 17 hours. The acid treatment enables the covalent attachment of chemical functional groups, such as hydroxyl (-OH) moieties, to CNT surfaces. This procedure results in the improvement of hydrophilicity as described in reference, [16]. It is also used in the purification process to remove metal particles and undesired substances after treating the metal surface by oxidation and sonication. The metal particle in the catalyst dissolves with acid treatment, while the nanotube remains as a suspended particle in the acid, [17].

Under these conditions, CNTs and other carbon-based particles show no observable modifications, whereas the metallic ones are dissolved or removed. Use of nitric acid as the agent has some features to advantages, including cheapness and high effectiveness for removing the metallic particles. However, the effect of hydrochloric acid treatment on the structures and properties of CNTs, [18], [19], [20] is little affected. The ultrasonic method involves the use of ultrasound waves to break up the very hard-to-separate nanotube clumps. The ultrasonication time is usually about 40-60 minutes. After the acid treatment, the solution was placed in a centrifuge process altitude speed of 10,000 rotations per minute for a duration of one hour to have the supernatant, [21]. The supernatant was then washed several times with deionized water until the pH of the solution was about 7. Subsequently, the CNTs obtained were dried in a furnace at 70 ºC for 72 hours. This process produced functionalized and purified carbon nanotube (O-CNT) powder.

2.3 Fabrication of Gas Sensor

To produce a Hydrogen gas sensor, a 100 nm thick Palladium (Pd) electrode finger was deposited on a PET using an RF magnetron sputtering system (A500 Edwards). The dimensions of the electrode fingers are as follows: width of 0.35 mm, length of 3.4 mm, and a space of 0.40 mm.

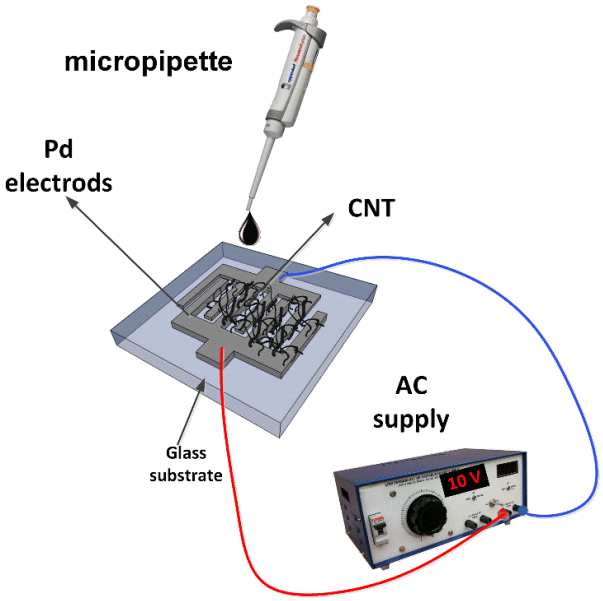

Fig. 2: Fabrication of MWCNT gas sensor using DEP
Source: [22]

A carbon nanotube (CNT) solution was prepared by dissolving 3 mg of MWCNTs (Microwave (MW) oven-synthesized CNTs, followed by oxidation of CNTs in HNO3 acid) in 20 ml of ethanol. The suspension of carbon nanotube (CNT) in the solution was prepared by sonication for 60 min. The CNTs were dispersed and stabilized very well by this structure. The concentration of CNT suspension was approximately 150 µg ml-1. A 0.5 µl volume of a carbon nanotube (CNT) solution was then carefully deposited between palladium (Pd) electrodes. This process was performed in the presence of an AC electric field (10 V, 50 Hz). A carbon-ethanol solution of about 10 µl was dropped onto the substrate between the electrodes with a micropipette, [22]. A schematic of the deposition of CNTs on a Pd electrode by AC dielectrophoresis is shown in Figure 2.

2.4 Experimental Sensing Set-Up

The gas-sensing studies of carbon nanotubes (CNTs) were carried out using hydrogen gas (H2). Such an assessment was performed by a commercially available sensor system that worked in connection with a Keithley 2400 source meter. The activity of the sensor was investigated by measuring the current-voltage curve with a fixed applied voltage of 0.05 V. The total flow rate of 1000 ppm was kept constant during the response measurement. The sensor was inserted into a

homemade box, and the two Pd-electrodes of the sensor were connected to a computer controlled by a Keithley 2400 source meter. Then the sensor was tested at room temperature to 1000 ppm of H_2 gas exposure. The composition of the main gases (H2/N2) and dry air was varied to control the H2 gas concentration via the two controllers of gas flow.

3 Result and Dissociation

3.1 FESEM and TEM Observation

The microwave irradiation process-formed carbon nanotubes (MW-CS-CNTs) show the presence of iron (Fe) catalyst nanoparticles filled inside the entire cavity and the upper or lower part of the CNTs (Figure 3). It has already been reported [23] that Fe nanoparticles are in a liquid state and are a frittered form of metal particles in the tube. Ferrocene decomposed under microwave irradiation, and Fe atoms were obtained. These atoms either meandered over the surface of the substrate before adhering to carbon nanotube roots, [24]. The Fe adhesion to as-prepared carbon nanotube walls is due to the relatively large capillary forces acting on the tube, [25]. In Figure 3, an individual carbon nanotube (CNT) with graphitic caps (GPC) and encapsulated iron (Fe) nanoparticles is shown oriented with respect to the CNT axis. The CNT diameters show little variation along their lengths as a result of iron nanoparticle accumulation during growth (Figure 3 (a)), [26].

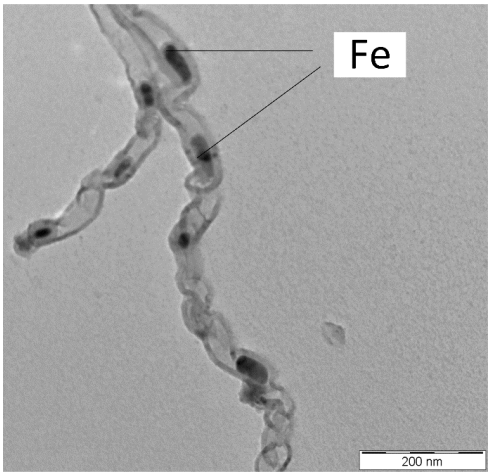

Fig. 3: TEM photo of CNT produced using a microwave oven from a ferrocen/graphite ratio of 30:70

The morphology between as-produced and functionalized shapes of CNTs was analyzed by FESEM, as shown in the Figure. 4. Amorphous C and Fe particles are discerned to be deposited on and inside the "as-grown" CNTs in Figure 4(a). On the contrary, significantly fewer amorphous carbon and iron particles were seen after nitric acid treatment, which was clearly shown in the Figure. 4(b).

The CNTs were analyzed by EDX, and the corresponding EDX results are illustrated in the Figure. 4(a) and (b) for those shown in the Figure 5(a) and (b), respectively. This was confirmed by the EDX results, which report the A-CNTs (Elemental analysis) (Table 1). The elemental composition of A-CNTs (in atomic percentage) determined by EDX analysis is given in Table 1, oxygen (O), carbon (C), and a small amount of iron (Fe) as observed in Table 1. Upon oxidation with HNO3 and purification treatments, the weight % of Fe in O-CNTs was reduced remarkably. In contrast, the mass fraction of oxygen was largely raised based on the functionalized carbon nanotubes (O-CNTs) compared to raw nanotubes.

The CNTs typically show bundled structures, as indicated in the FESEM images (as reported previously, [27], [28]. On the one hand, CNTs are more soluble in ethanol after oxidizing by nitric acid. Even in the absence of surfactants or polymerization, this enhancement occurs because a small amount of functionality is being integrated. Oxidation of the CNTs leads to partial disentangling of bigger diameter bundles into smaller diameter bundles and individual tubes (Figure 4(b)–FESEM images).

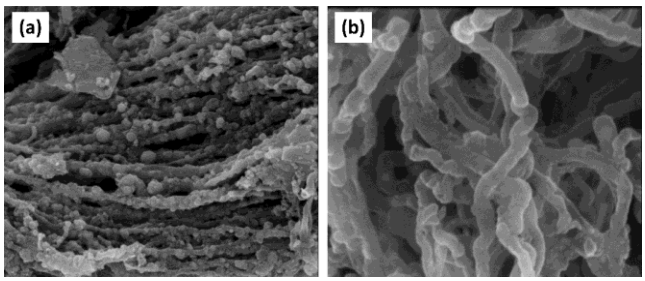

Fig. 4: FESEM for (a) as-produced CNT, and (b) CNT after purification

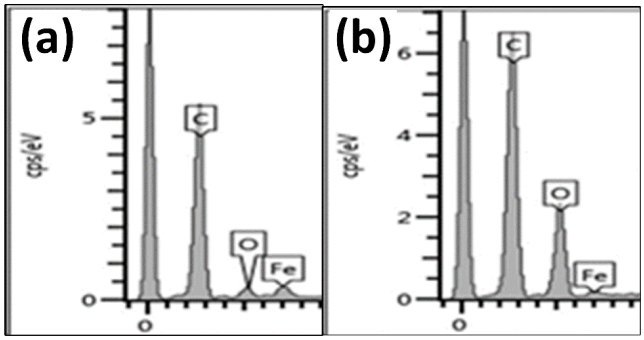

Fig. 5: (a) EDX analysis of CNT after purification, (b) EDX analysis of as-produced CNT

TEM image of purified CNTs by HNO3 treatment is shown in the Figure 6. The results indicate that large amounts of the iron particles at the tips of the CNTs are etched away. The metal wood catalyst was potentially removed when the complex was opened with nitric acid. It is also well known in the art that nitric acid (HNO3) is effective at removing metal particles. This is a result of its strong oxidizing properties that make it capable of removing amorphous carbon, [23].

Table 1. The Energy Dispersive X-ray (EDX) analysis was performed on both the as-produced Carbon nanotubes (A-CNT) and the CNT after purification (O-CNT)

Element	Weight%	
	A-CNT	O-CNT
C	71	64
O	5.2	32
Fe	24	4.3

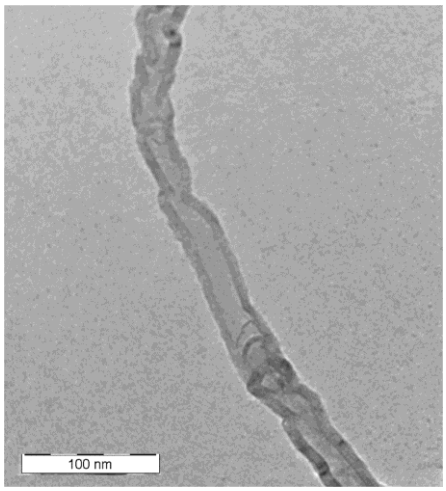

Fig. 6: TEM image of carbon nanotubes (CNTs) following their purification process

3.2 Raman Spectroscopy Analysis

Figure 7 shows the Raman spectrum for the as-synthesized CNTs and purified CNTs. Four bands appear at a wavenumber of 1330 cm-1 and could be attributed to the presence of defects (D) in the hexagonal carbon lattice of the sp2 graphene layer. Furthermore, another band appears at 1580 cm-1 due to well-ordered carbon atoms of the graphitic (G) structure. Also, a two-dimensional active band of CNTs with certain chirality conditions by double resonance was observed. The ID/IG intensity ratio for carbon nanotubes (CNTs) is employed to evaluate the extent of the ordered structure and presence of disorder, [29]. It is an indicator of the quality of the crystallinity of the phase in the samples studied. The CNT ID/IG ratio implies a well-organized graphitic structure of CNTs. The sensitivity of the carbon nanotubes (CNTs) 2D peak to an increase in the defects' density has been verified, and the I2D/ID ratio has been used as the measurement metric for the crystallinity quality and phase purity factor of the CNTs studied, [30].

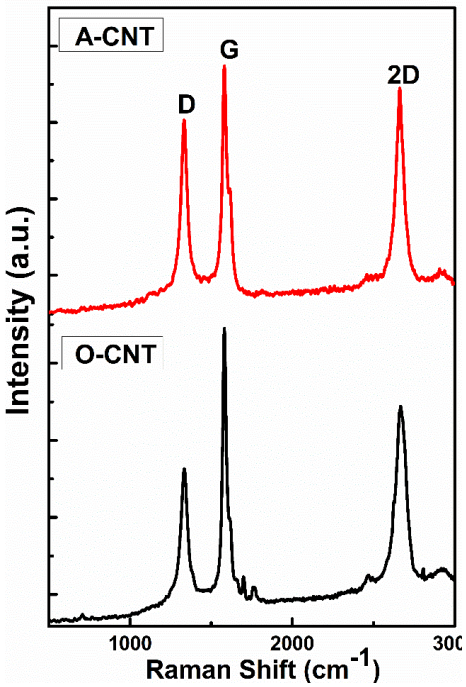

Fig. 7: The Raman spectra of A-CNT (as-produced CNT) and O-CNT (purified CNT)

The Raman spectra of carbon nanotubes in their as-prepared state (referred to as A-CNT) and after functionalization (referred to as O-CNT) were analyzed.

Table 2 lists the intensity ratio of the Raman bands and the FWHM for A-CNT and O-CNT. The ID/IG ratio and FWHM of the G band indicate a decrease of 34 and 0.59, respectively, for O-CNTs when compared to CNTs synthesized under standard conditions. Furthermore, the I2D/ID ratio for O-CNTs showed a 1.31 times increase compared with as-synthesized CNTs. Typically, the Raman peak ratios (ID/IG) exhibit a reduction after the purification step, as the removal of amorphous carbon enhances nanotube concentration. Additionally, the ID/IG ratio is observed to be directly related to the amount of disordered carbon in the graphitic material sample. The reduced ID/IG and FWHM G ratios, alongside the higher I2D/ID ratio for O-CNTs, indicate the transfer of oxidized amorphous carbon to the centrifuged suspension. As a result, this approach led to the formation of highly crystalline graphite pieces, polyhedral carbon, some small Fe particles, and a few large CNT bunches in the sediment collected after centrifugation.

Table 2. A comparative analysis of the intensities of Raman bands and the full width at half maximum (FWHM) G for both A-CNTs and O-CNTs

properties	A-CNT	O-CNT
I_D/I_G	0.81	0.59
I_{2D}/I_D	1.12	1.31
FWHM G	38	34
L_a (nm)	15.6	25.7

The equation from Cancado et al. was used to calculate the crystallite size (La) of nanographitic from the Raman spectrum, [31]. The equation (1) can be expressed as:

$$L_a(nm) = \frac{560}{E_L^4}\left(\frac{I_D}{I_G}\right)^{-1} \quad (1)$$

where E_L represents the excitation laser energy employed in Raman spectroscopy with a value of 1.96 eV. Table 2 demonstrates an increase in crystallite size from 15.6 nm for A-CNT to 25.7 nm for O-CNT.

3.3 FTIR Observation Analysis

Figure 8 shows the FTIR spectra of the CNTs in as-synthesized and after functionalization. The existence of -OH groups, on the surface or sorbed water, and carboxyl groups is indicated by the strong absorption peak at 3553 cm-1. The bands in the range 1550–1750 cm-1 may be attributed to the inversion of the C-C bond in aromatic rings and C-O in groups in different compounds such as ketones, quinones, and carboxylic acids. On the other hand, absorbance bands located in the 950–1300 cm-1 region correspond to C-O bond vibrations in various chemical environments, [32], [33]. The peak at 1406 cm-1 could be due to the hydroxyl (OH) groups of the sorbed water, or an overlapped band of carbon-oxygen (C-O) functional group.

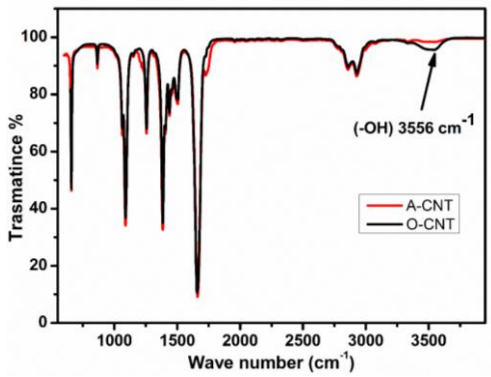

Fig. 8: The FTIR spectra of as-produced (A-CNT) and after functionalization (O-CNT)

The absorption peaks at 2930 cm-1 and 1385 cm-1 are characteristic bands of hydroxyl groups (OH) resulting from the synthesis procedure of carbon nanotube, [34]. The -OH band at 3556 cm-1 was weakened by CNT functionalization. Figure 8 shows FTIR spectra of fluorinated carbon nanotubes (O-CNTs) show that they contain different hydroxyl groups attached to the sidewalls of the CNTs, [35], [36].

3.4 Electrical Properties

The electrical behaviour of A-CNTs and O-CNTs sensors was measured with the voltage from -5 V to +5 V, as shown in Figure 9. The current of O-CNTs reached 35 mA at 5 V, but that of A-CNTs only reached 11 µA. The electrical transport properties of the CNTs functionalized are much higher than those of the non-functionalized CNTs, which is significantly higher, at least by about a thousand times. Functionalized carbon nanotubes have functional groups on their surface, and this leads to a high density of states in the vicinity of the Fermi surface. This higher density promotes the transfer of electrons between the carbon atoms, [36].

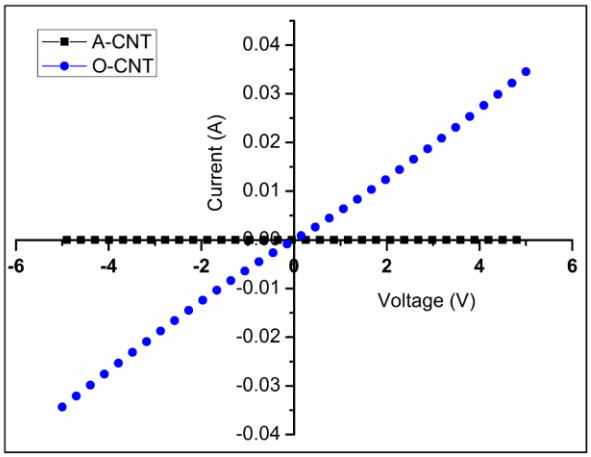

Fig. 9: Comparison of I-V characteristics of A-CNTs and O-CNTs at 5V

3.5 Gas Sensor Properties

The CNT-based hydrogen gas sensor was placed in a chamber at room temperature. The gas-sensing characteristics were evaluated by controlling the hydrogen (H2) concentration with a mass flow controller (MFC). Concurrently, the flow rate of the gas mixture was set to be 1000 ppm. The sensitivity of the sensor is based on the relative change in its electrical resistance, which can be described by the equation, [37]:

$$\text{Sensitivity } (\%) = \frac{R_{gas} - R_{air}}{R_{air}} \times 100 \quad (2)$$

Here, R_{gas} represents the minimum resistance of CNTs in H2 atmosphere, while R_{air} represents the maximum resistance of CNTs in air atmosphere.

The aforementioned expression can also be formulated in relation to the electrical current generated in carbon nanotubes (CNTs) when subjected to a direct current (DC) bias voltage, [38]. The sensitivity percentage can be calculated using the following formula:

$$\text{Sensitivity } (\%) = \frac{I_{gas} - I_{air}}{I_{air}} \times 100 \quad (3)$$

Herein, Igas represents the maximum current recorded following exposure to H2, while Iair represents the current measured in a pure air environment.

From the above equations, it is easy to find that the sensor sensitivity is related to the amount of electron charge transfer and surface interaction between gas and CNTs. Moreover, it is important to note that carbon nanotubes (CNTs) have four possible adsorbing sites for H2 gas molecules: inside, interstitial channels, external grooves, and external surface, [39].

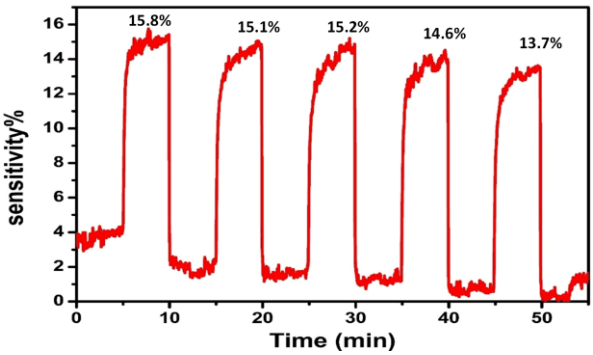

Fig. 10: Sensitivity and cyclic response of CNTs-based gas sensor when exposed to H2 gas (1000 ppm) at RT

The sensitivity of the gas sensor (C-O-CNTs) described by Equation (2) based on the carbon nanotubes is shown in Figure 10 at RT as a function of the applied voltage at a value of 0.05 V. This means, by these curves, the influence of the applied voltage to the sensor sensitivity at RT, when it was exposed to a concentration value of 1000 ppm at RT. Under the present working conditions, the devices show good repeatability and very high sensitivity of up to 15% when they were exposed to 1000 ppm concentration of H2/balance N2 gas at room temperature.Comparison of Gas Detection Properties of the A-CNT Sensor and O-CNT Sensor. The comparison results of the gas detection properties of the A-CNT-based and O-CNT-based sensors are shown in Table 3. In their analysis, 1000 ppm H2 gas concentration at RT is particularly considered. The recorded rise time of the response (at RT) for A-CNT and O-CNT was found to be 2 and 1.45 s, respectively. As for the response time of the characteristic curve (at a concentration of 1000 ppm at RT), substrates O-CNT and A-CNT were measured to be 30 and 34 seconds, respectively. Such results have proven that the sensor response of the detected H2 gas molecules of this sensor (the detecting response of H2 gas molecules: S) was faster than that of this sensor (S was the sensing response of the sensors and shown in Table 3).

Table 3. A comparative analysis of gas sensor properties for both A-CNTs and O-CNTs

Gas sensor properties	A-CNT	O-CNT
Sensitivity%	10.7	15
Rise time (s) ±0.05	2	1.45
Fall time (s) ± 0.05	34.4	29.5

The increase in the rise and fall times of the O-CNT sensor is mainly caused by the surface functionalization after acid treatment. This process provides more adsorption channels for H2 molecules on the large surface, and the capacity of molecular adsorption at the surface dangling bonds is enhanced. In addition, the observed improvement in the hydrogen gas sensing response of the functionalized carbon nanotube (O-CNT) based response may also be related to the gas molecules dissociation mechanism into hydrogen atoms taking place at the edges of the functionalized carbon nanotubes. Surface functionalized oxidation CNTs with -COOH, -OH, and C-O functional groups of the aromatic ring have higher activity. Therefore, the active site of functional chemical groups on the surface of CNTs acted as a catalyst to enhance the dissociation of H2 molecules into H atoms. Hydrogen gas molecules are assumed to be adsorbed into four possible sites on the fluorinated carbon nanotubes (O-CNTs) as shown in the image (red blobs). In a recent study conducted in [36], it turned out to be possible to detect H2 gas with multi-walled carbon nanotubes (MWCNTs) functionalized. The detection limit of this detection mechanism is as low as 0.8% for a 500 ppm H2 concentration, at room temperature. The detection recovery time was found to be 100s.

The developed sensor, employing MWCNTs, shows remarkable response and better sensitivity of pristine MWCNTs and sensing capability towards H2 gas at RT. This improvement compares with the results of previous studies (Table 4, Appendix). The response of the sensor toward H2 gas was found to

have a rise time of 29 s at RT. This means that the sensor has a quick response to H2 gas as fast as several tens of seconds. This fast response of the hydrogen gas sensor using carbon nanotubes (CNTs) may be due to the large surface-to-volume ratio of the CNTs. This property increases the amount of hydrogen adsorption sites and promotes the migration of hydrogen molecules within the CNTs. If the test gas is replaced with air, the gas sensor recovers to its initial state immediately. A present CNT gas sensor exhibits a recovery time of 1.45 s at room temperature (RT). This recovery time is significantly shorter than the recovery times for other CNT-based sensors measured in previous works, [40], [41], [42].

As can be seen in the inset, the repeatability of the sensor to low H2 concentration (1000 ppm) indicates that the sensitivity of the sensor is reproducible for multiple exposures to H2. It means that the sensor has reproducible sensing properties. In comparison with the works reported recently, the performance of the proposed sensors in terms of operation temperature, sensor types, response, and gas concentration is systematically compared in Table 4 (Appendix). It has been validated from the results that the suggested CNT-O-based hydrogen gas sensor has better output characteristics than other improved sensors by other authors.

The noteworthy property of increased conductivity with higher H2 adsorption and decreased conductivity in the absence of H2 and exposure to air should be highlighted. This behaviour can only be produced by n-type charge carriers in the carbon nanotube (CNT). This finding contradicts previous studies that asserted the p-type nature of CNTs. The following is a detailed explanation of this matter: The carbon nanotubes (CNTs) located between the two palladium (Pd) electrodes consist of a mixture of semiconducting and metallic CNTs.

The current in the sensitive material is primarily regulated by the metallic tube due to its low resistance, [43], [44].

The increased conductivity observed in a carbon nanotube (CNT)-based gas sensor upon exposure to a low concentration of hydrogen gas can be explained as follows: It is believed that H2 molecules function as a reducing agent by transferring a single electron to carbon nanotubes (CNTs). Hydrogen gas (H2) can function as an electron donor to carbon nanotubes (CNTs) in the current gas sensor. Consequently, upon exposure to H2 gas, a transfer of electrons will occur from H2 to CNTs. This procedure has been shown to effectively enhance the electron count, resulting in a reduction in carbon nanotube (CNT) resistance and an improvement in conductivity, as demonstrated in previous studies, [40], [45], [46]. During the reverse process, in the presence of oxygen, the adsorbed atomic H2 undergoes a reaction with O2 to produce hydroxyl groups. These hydroxyl groups subsequently combine with the adsorbed H2 to form water, which can then be released from the carbon nanotube-based sensor. Therefore, oxygen present in the atmosphere catalyzes the restoration of carbon nanotube (CNT) surfaces. When the flow of H2 gas is discontinued, the process exhibits sensor reversibility, enabling the restoration of the electrical properties of carbon nanotubes (CNTs), [38], [47], [48].

Figure 11 illustrates a proposed mechanism for the adsorption of H2 gas molecules onto the surface of functionalized carbon nanotubes (F-CNTs), emphasizing four critical interaction sites: internal pores, external grooves, interstitial channels, and outer surfaces. The observed enhancements in rise and fall times in the F-CNT-based sensor can be chiefly ascribed to the surface functionalization attained via acid treatment. This process enhances the density of active sites across the extensive surface area, thereby increasing the adsorption capacity of H2 molecules at surface dangling bonds, [17], [49].

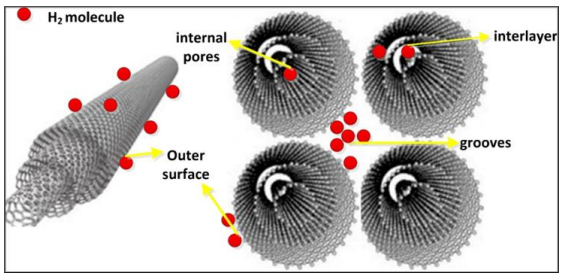

Fig. 11: Schematic of H_2 adsorption and dissociation on acid-functionalized CNTs (F‑CNTs)
Source: [49]

Additionally, the dissociation of H_2 molecules into atomic hydrogen at the reactive edges of the nanotubes is responsible for the enhanced hydrogen gas sensing capability of the functionalized carbon nanotube (F-CNT) sensor. Functional groups like -COOH, -OH, and C-O are added to the aromatic rings of a carbon nanotube (CNT) when its surface oxidizes. The CNTs' chemical activity increases significantly as a result (Figure 11). The observed improvements in rise and fall times in the F-CNT-based sensor can primarily be attributed to the surface functionalization achieved through acid treatment. This process enhances the density of active sites across the extensive surface area,

thereby increasing the adsorption capacity of H_2 molecules at surface dangling bonds, [7].

4 Conclusion

The O-CNT was employed for the preparation of novel, highly sensitive, efficient, and economic CNT-based hydrogen gas sensors. This was realized by an easily fabricated dielectrophoresis deposition process for CNTs on PET substrates. The p-type property of CNTs has been reported to be due to the presence of a metallic CNT network that hinders the current flow throughout CNT-based gas sensors. The sensor had a relatively high sensitivity of about 15% to the hydrogen (H2) concentration of 1000 ppm at room temperature (RT). Additionally, the sensor had a fast response and recovery time (about 1.45 and 30 s). It was reported with great effectiveness that innovative CNT-based nanostructures were utilized in gas sensing for highly sensitive detections of low concentrations of H2 at room temperature (RT). That will pave the way for high-performance H2 gas sensors with great efficiency. Two gas sensors based on untreated A-CNT and acid-treated O-CNT were tested and compared with the results from similar works reported in the literature. The sensing characteristics of the sensors were analysed in terms of their response, response time, and recovery time to RT and H2 gas at 1000 ppm. The O-CNT sensor has a higher sensing capability than the A-CNT sensor for the whole gas concentration containing RT. The recovery and rise time of the O-CNT sensor was found to be smaller than compared of the A-CNT sensor. The improved gas-sensitive performance of the O-CNT-based sensor is likely thanks to the fact that many hydroxyl groups and other chemical functional groups have been attached to the surface of CNTs. These surface-active sites adsorb several H2 gas molecules and dissociate into hydrogen atoms. Means have been included for sensing gas. It was revealed that these functional groups are catalytic centres for chemisorption and subsequent dissociation of H2 gas molecules. This was attributed to the increased crystallite sizes of CNTs, which had allowed a bigger ability to adsorb H2 on the fluorinated CNT (O-CNT). The O-CNT on PET-based sensor has shown a remarkable dynamic response of 15% at room temperature, which is almost equivalent to the highest value reported so far in the available literature of H2 gas sensors based on CNT. Good gas sensors are known to be based on the functionalization of the surface of carbon nanotube (CNT).

Acknowledgements:
The authors are grateful to Al-Zaytoonah University of Jordan and Isra University, Amman, Jordan. For the help and support in the achievement of this research project.

References:

[1] Collins, P.G., et al., Extreme oxygen sensitivity of electronic properties of carbon nanotubes. *Science,* 2000. 287(5459): p. 1801-4. doi: 10.1126/science.287.5459.1801.

[2] Kong, J., et al., Nanotube molecular wires as chemical sensors. *Science,* 2000. 287(5453): p. 622-625. doi: 10.1126/science.287.5453.622.

[3] Yang, X., et al., Effect of carbon nanotube (CNT) content on the properties of in-situ synthesis CNT reinforced Al composites. *Materials Science and Engineering:* A, 2016. 660: p. 11-18. doi: 10.1016/j.msea.2016.02.062.

[4] Wang, Y. and J.T. Yeow, A review of carbon nanotubes-based gas sensors. *Journal of sensors,* 2009. 2009(1). doi: 10.1155/2009/493904.

[5] Aljohani, F.S., et al., Water Treatment from MB Using Zn-Ag MWCNT Synthesized by Double Arc Discharge. *Materials* (Basel), 2021. 14(23): p. 7205. doi: 10.3390/ma14237205.

[6] Dai, J., et al., Printed gas sensors. *Chemical Society Reviews,* 2020. 49(6): p. 1756-1789. doi: 10.1039/C9CS00459A.

[7] Zidan, M., et al., Voltammetric reduction of Ellagic acid nanocomposite Using Carbon nanotube-Modified Glassy Carbon Electrode. *Journal of Pure & Applied Sciences,* 2018. 17(1). doi: 10.51984/jopas.v17i1.188.

[8] Peng, N., et al., Sensing mechanisms for carbon nanotube based NH3 gas detection. *Nano letters,* 2009. 9(4): p. 1626-1630. doi: 10.5772/39433.

[9] M. Y. Hariyawan, M.Y.H., A.G. A. Gunawan, and E.H.P. E. H. Putra, Wireless Sensor Network for Forest Fire Detection. *TELKOMNIKA (Telecommunication Computing Electronics and Control),* 2013. 11(3): p. 563. doi: 10.12928/telkomnika.v11i3.1139.

[10] Hübert, T., et al., Hydrogen sensors–a review. Sensors and Actuators B: *Chemical,* 2011. 157(2): p. 329-352. doi: 10.1016/j.snb.2011.04.070.

[11] Lin, L., et al., Fabrication of highly stretchable conductors via morphological control of carbon nanotube network. *Small,* 2013. 9(21): p. 3620-3629. doi: 10.1002/smll.201202306.

[12] Li, Y. and H. Shimizu, Toward a Stretchable, Elastic, and Electrically Conductive Nanocomposite: Morphology and Properties of Poly[styrene-b-(ethylene-co-butylene)-b-styrene]/Multiwalled Carbon Nanotube Composites Fabricated by High-Shear Processing. *Macromolecules,* 2009. 42(7): p. 2587-2593. https://doi.org/10.1021/ma802662c.

[13] Yan, K., et al., Fabrication of multiwall carbon nanotube sheet based hydrogen sensor on a stacking multi-layer structure. *Nanotechnology,* 2018. 29(37): p. 375503. doi: 10.1088/1361-6528/aace96.

[14] Shrivastava, S., et al., Effect of MWNT concentration on hydrogen gas sensing property of MWNT-ployaniline composite. *International Journal of Hydrogen Energy,* 2022. 48(96): p. 38107-38117. doi: 10.1016/j.ijhydene.2022.12.053.

[15] Algadri, N.A., et al., Cost-effective single-step carbon nanotube synthesis using microwave oven. *Materials Research Express,* 2017. 4(8): p. 085602. doi: 10.1088/2053-1591/aa817b.

[16] Kumar, M.K. and S. Ramaprabhu, Palladium dispersed multiwalled carbon nanotube based hydrogen sensor for fuel cell applications. *International Journal of Hydrogen Energy,* 2007. 32(13): p. 2518-2526. doi: 10.1016/j.ijhydene.2006.11.015.

[17] Santangelo, S., et al., Effect of sulphuric–nitric acid mixture composition on surface chemistry and structural evolution of liquid-phase oxidised carbon nanotubes. *Journal of Raman Spectroscopy,* 2012. 43(10): p. 1432-1442. doi: 10.1002/jrs.4097.

[18] Tao, Zhizhi, et al., "Recent Advances in Carbon Nanotube Technology: Bridging the Gap from Fundamental Science to Wide Applications," C, vol. 10, no. 3, p. 69, 2024, doi: 10.3390/c10030069.

[19] Wepasnick, K.A., et al., Surface and structural characterization of multi-walled carbon nanotubes following different oxidative treatments. *Carbon,* 2011. 49(1): p. 24-36. doi: 10.1016/j.carbon.2010.08.034.

[20] Hu, H., et al., Nitric acid purification of single-walled carbon nanotubes. *The Journal of Physical Chemistry B,* 2003. 107(50): p. 13838-13842.

[21] Yu, A., et al., Application of centrifugation to the large-scale purification of electric arc-produced single-walled carbon nanotubes. *J Am Chem Soc,* 2006. 128(30): p. 9902-8. doi: 10.1021/ja062041m.

[22] Algadri, N.A., et al., A High-Sensitivity Hydrogen Gas Sensor Based on Carbon Nanotubes Fabricated on Glass Substrate. *Journal of Electronic Materials,* 2018. 47(11): p. 6671-6680. doi: 10.1007/s11664-018-6537-6.

[23] Chen, X., et al., TEM investigation on the growth mechanism of carbon nanotubes synthesized by hot-filament chemical vapor deposition. *Micron,* 2004. 35(6): p. 455-460. https://doi.org/10.1016/j.micron.2004.02.006.

[24] Amama, P.B., et al., Role of water in super growth of single-walled carbon nanotube carpets. *Nano Lett,* 2009. 9(1): p. 44-9. doi: 10.1021/nl801876h.

[25] Ajayan, P.M., Capillarity-induced filling of carbon nanotubes. *Nature,* 1993. 361(6410): p. 333-334. https://doi.org/10.1038/361333a0.

[26] Bajpai, R. and H.D. Wagner, Fast growth of carbon nanotubes using a microwave oven. *Carbon,* 2015. 82: p. 327-336. doi: 10.1016/j.carbon.2014.10.077.

[27] Wick, P., et al., The degree and kind of agglomeration affect carbon nanotube cytotoxicity. *Toxicol Lett,* 2007. 168(2): p. 121-31. doi: 10.1016/j.toxlet.2006.08.019.

[28] Vignes, A., et al., Thermal ignition and self-heating of carbon nanotubes: From thermokinetic study to process safety. *Chemical Engineering Science,* 2009. 64(20): p. 4210-4221. doi: 10.1016/j.ces.2009.06.072.

[29] Brown, S., et al., Observations of the D-band feature in the Raman spectra of carbon nanotubes. *Physical Review B,* 2001. 64(7): p. 073403. doi: 10.1103/PhysRevB.64.073403.

[30] Żelechowska, K., et al., Oxygen biosensor based on carbon nanotubes directly grown on graphitic substrate. *Sensors and Actuators B: Chemical,* 2017. 240: p. 1308-1313. doi: 10.1016/j.snb.2016.09.081.

[31] Cançado, L., et al., General equation for the determination of the crystallite size L a of nanographite by Raman spectroscopy. *Applied Physics Letters,* 2006. 88(16): p. 163106. doi: 10.1063/1.2196057.

[32] Stobinski, L., et al., Multiwall carbon nanotubes purification and oxidation by nitric acid studied by the FTIR and electron

spectroscopy methods. *Journal of Alloys and Compounds,* 2010. 501(1): p. 77-84. doi: 10.1016/j.jallcom.2010.04.032.

[33] Tchoul, M.N., et al., Effect of mild nitric acid oxidation on dispersability, size, and structure of single-walled carbon nanotubes. *Chemistry of Materials,* 2007. 19(23): p. 5765-5772. doi: 10.1021/cm071758l.

[34] Kang, S.-Z., et al., A facile preparation of multiwalled carbon nanotubes modified with hydroxyl groups and their high dispersibility in ethanol. Colloids and Surfaces A: *Physicochemical and Engineering Aspects,* 2011. 384(1): p. 363-367. doi: 10.1016/j.colsurfa.2011.04.036.

[35] Zhang, J., et al., Effect of Chemical Oxidation on the Structure of Single-Walled Carbon Nanotubes. *The Journal of Physical Chemistry B,* 2003. 107(16): p. 3712-3718. doi: 10.1021/jp027500u.

[36] Dhall, S., N. Jaggi, and R. Nathawat, Functionalized multiwalled carbon nanotubes based hydrogen gas sensor. *Sensors and Actuators A: Physical,* 2013. 201: p. 321-327 doi: 10.1016/j.sna.2013.07.018.

[37] Buttner, W.J., et al., An overview of hydrogen safety sensors and requirements. *International Journal of Hydrogen Energy*, 2011. 36(3): p. 2462-2470. doi: 10.1016/j.ijhydene.2010.04.176.

[38] Kadhim, I.H. and H.A. Hassan, Room temperature hydrogen gas sensor based on nanocrystalline SnO2 thin film using sol–gel spin coating technique. *Journal of Materials Science: Materials in Electronics,* 2016. 27(5): p. 4356-4362. doi: 10.1007/s10854-016-4304-0.

[39] Zhao, J., et al., Gas molecule adsorption in carbon nanotubes and nanotube bundles. *Nanotechnology,* 2002. 13(2): p. 195-200. doi: 10.1088/0957-4484/13/2/312.

[40] Kumar, M.K., A.L.M. Reddy, and S. Ramaprabhu, Exfoliated single-walled carbon nanotube-based hydrogen sensor. *Sensors and Actuators B: Chemical,* 2008. 130(2): p. 653-660. doi: 10.1016/j.snb.2007.10.033.

[41] Kong, J., M.G. Chapline, and H. Dai, Functionalized carbon nanotubes for molecular hydrogen sensors. *Advanced Materials,* 2001. 13(18): p. 1384-1386. doi: 10.1002/1521-4095(200109)13:18<1384::AID-ADMA1384>3.0.CO;2-8.

[42] Majumdar, S., P. Nag, and P.S. Devi, Enhanced performance of CNT/SnO 2 thick film gas sensors towards hydrogen. *Materials Chemistry and Physics,* 2014. 147(1): p. 79-85. doi: 10.1016/j.matchemphys.2014.04.009.

[43] An, K.H., et al., Enhanced Sensitivity of a Gas Sensor Incorporating Single-Walled Carbon Nanotube–Polypyrrole Nanocomposites. *Advanced Materials,* 2004. 16(12): p. 1005-1009. doi: 10.1002/adma.200306176.

[44] Vijayaraghavan, A., et al., Metal− semiconductor transition in single-walled carbon nanotubes induced by low-energy electron irradiation. *Nano letters,* 2005. 5(8): p. 1575-1579. doi: 10.1021/nl0509935.

[45] Ding, D., et al., Hydrogen sensors based on aligned carbon nanotubes in an anodic aluminum oxide template with palladium as a top electrode. *Sensors and Actuators B: Chemical,* 2007. 124(1): p. 12-17. doi: 10.1016/j.snb.2006.11.034.

[46] Guo, K. and A.H. Jayatissa, Hydrogen sensing properties of multi-walled carbon nanotubes. *Materials Science and Engineering: C,* 2008. 28(8): p. 1556-1559. doi: 10.1016/j.msec.2008.04.014.

[47] Abdullah, Q.N., et al., High performance room temperature GaN-nanowires hydrogen gas sensor fabricated by chemical vapor deposition (CVD) technique. *International Journal of Hydrogen Energy,* 2013. 38(32): p. 14085-14101. doi: 10.1016/j.ijhydene.2013.08.014.

[48] Mubeen, S., et al., Palladium nanoparticles decorated single-walled carbon nanotube hydrogen sensor. *The Journal of Physical Chemistry C,* 2007. 111(17): p. 6321-6327. doi: 10.1021/jp067716m.

[49] Al-Diabat, A.M., et al., Improved Hydrogen Gas Sensing Performance of Carbon Nanotube Synthesized Using Microwave Oven. *IEEE Sensors Journal,* 2023. 23(2): p. 1033-1041. doi: 10.1109/jsen.2022.3226042.

APPENDIX

Table 4. compares this study and some previous studies

Sensor type	Gas concentration (ppm)	Sensitivity (%)	Response /recovery time(s)	Operating temperature (ºC)	Reference
SWCNT&Pd	40000	9	560/560	RT	[16]
MWCNT	500	0.8	/100	RT	[36]
MWCNT	1000	15	179/19	RT	This work
SWCNT&Pd	40000	15	600/840	RT	
MWCNT & Pd	2100	2.15	198/-	RT	[40]
	70	0.60	270/-	RT	[43]
CNT	1000	0.58	560/-	RT	[44]
	100	6	-/-	RT	
CNT & Pd	2100	2.15	198/210	RT	[43]
MWCNT	18000	13	20/-	100	[45]
MWCNT	1000	2	-/-	RT	[46]
	1000	6.5	-/-	300	
MWCNT	4000	12.3	200/-	RT	[13]
MWCNT	500	2.1	15/-		[14]

Contribution of Individual Authors to the Creation of a Scientific Article (Ghostwriting Policy)

- Ahmad M. Al-Diabat (first author, corresponding author) conceived the research idea, developed the theoretical framework, supervised all stages of the work, contributed to data analysis, and led the writing of the final manuscript.
- Natheer A. Algadri contributed to the experimental design, performed physical calculations, and participated in the interpretation of theoretical results.
- Naser M. Ahmed conducted laboratory experiments, collected data, and assisted in data analysis.
- Tariq AlZoubi participated in the literature review and analyzed results using programming and simulation tools.
- Ghaseb N. Makhadmeh developed the physical models used in the research and verified theoretical calculations.
- Abdulsalam Abuelsamen contributed to editing and drafting the experimental sections and the results.
- Osama Abu Noqta organized data and prepared tables and figures.
- Amal Mohamed Ahmed Ali was responsible for language proofreading, compliance with academic publishing standards, and final manuscript revision before submission.

Sources of Funding for Research Presented in a Scientific Article or Scientific Article Itself

No funding was received for conducting this study.

Conflict of Interest

The authors have no conflicts of interest to declare that are relevant to the content of this article.

Creative Commons Attribution License 4.0 (Attribution 4.0 International, CC BY 4.0)

This article is published under the terms of the Creative Commons Attribution License 4.0
https://creativecommons.org/licenses/by/4.0/deed.en_US